JAIST Repository
https://dspace.jaist.ac.jp/

Title	Binding Energy of the Electron-Hole Liquid in Type-II (GaAs)_m/(AlAs)_m Quantum Wells
Author(s)	Inagaki, Akira; Katayama, Shin'ichi
Citation	Journal of the Physical Society of Japan, 72(6): 1452-1457
Issue Date	2003
Type	Journal Article
Text version	author
URL	http://hdl.handle.net/10119/4778
Rights	This is the author's version of the work. It is posted here by permission of The Physical Society of Japan. Copyright (C) 2003 The Physical Society of Japan. Akira Inagaki and Shin'ichi Katayama, Journal of the Physical Society of Japan, 72(6), 2003, 1452-1457. http://jpsj.ipap.jp/link?JPSJ/72/1452/
Description	

JAIST
JAPAN ADVANCED INSTITUTE OF SCIENCE AND TECHNOLOGY

Japan Advanced Institute of Science and Technology

Binding Energy of the Electron-Hole Liquid in Type-II $(GaAs)_m/(AlAs)_m$ Quantum Wells

Akira INAGAKI and Shin'ichi KATAYAMA*

School of Materials Science, Japan Advanced Institute of Science and Technology, 1-1 Asahidai, Tatsunokuchi, Ishikawa 923-1292

(Received March 22, 2003)

The binding energy of quasi-two-dimensional electron-hole liquid (EHL) at zero temperature is calculated for type-II $(GaAs)_m$ $/(AlAs)_m$ $(5 \leq m \leq 13)$ quantum wells (QWs). The correlation energy is evaluated by adopting a random phase approximation of Hubbard. For comparison, we calculate the binding energy of EHL for type-I $(GaAs)_m/(AlAs)_m$ $(14 \leq m \leq 20)$ QWs. It is demonstrated that the EHL in type-II GaAs/AlAs QWs is more stable state than exciton and biexciton at high excitation density, while the EHL is unstable in type-I GaAs/AlAs QWs.

KEYWORDS: semiconductor, quantum wells, type-II structure, electron-hole liquid, binding energy

* E-mail: s-kata@jaist.ac.jp

1. Introduction

The metallic electron-hole liquid (EHL) has attracted our attentions for a long time as an appearance of new condensed phase[1-3] in bulk semiconductors such as Ge and Si since the prediction by Keldysh.[4] Recent advance in both a noble ultrafast laser technique and a thin film growth method has opened a new stage of research for the EHL in semiconductors. The progress of mid-infrared pump-probe spectroscopy with high power laser reveals quite recently the existence of metastable EHL in direct-gap semiconductor CuCl.[5] They have also found very high critical EHL temperature (165 K) of diamond by using the time-resolved luminescence measurements.[6] Associated with new techniques in the crystal growth such as molecular-beam-epitaxy (MBE) method is a confinement of the EHL in semiconductor quantum-wells (QWs).[7,8] The high optical excitation effects such as a band-gap renormalization and a stability of quasi-two-dimensional (2D) EHL have been studied experimentally[8] and theoretically[9,10] in type-I QWs in which electrons and holes are located in the same confinement layers. The short-period $(GaAs)_m/(AlAs)_m$ ($m \leq 13$) superlattices exhibit type-II structure in which electrons and holes are separated spatially.[11] The formation of EHL in type-II GaAs/AlAs QWs is expected much because of the spatial separation of electron and hole, in addition to the indirect nature of energy gap in k-space as in Ge and Si. Such favorable condition to observe EHL stimulates intensive photoluminescence studies under high excitations so far.[12,13] Recently, the evidence of exciton condensation in GaAs/AlAs coupled QWs has been observed in photoluminescence and transport measurements in a strong magnetic field.[14,15] Lerner and Lozovik[16] and Kuramoto and Horie[17] have suggested theoretically that the critical condition for exciton condensation in QWs is enhanced by applying a magnetic field perpendicular to the 2D plane. It is quite intriguing that evidences of both EHL and exciton condensation have arisen in photoluminescence spectra from GaAs/AlAs QWs with high density ($\sim 10^{12}$ cm^{-2}) and low density ($\leq 10^{10}$ cm^{-2}) of electron-hole (e-h) pairs, respectively.

Theoretical study of the liquid phase in type-II structures[18] with high e-h pair-density is still scarce, because it seems that the correlation energy calculation requires the numerous effort. One of the persuasive method to calculate the correlation energy of EHL in previous studies is to adopt a random phase approximation (RPA) of Hubbard.[19] First attempt to evaluate the correlation energy in a RPA of Hubbard in bulk Ge and Si was done by Brinkman and Rice.[20] Their results have led to a stable EHL and were in good agreement with experiments for the equilibrium density and the binding energy. Kuramoto and Kamimura[21] have adopted this approximation for the correlation energy calculation for the layer-type semiconductors in the limit of 2D, and further Kleinman[9] has studied the correlation energy in RPA of Hubbard for type-I QWs with finite width, using the effective modeled Coulomb interaction among electrons, holes and between electron and hole.

In this paper we present the ground state energy calculation of quasi-2D EHL in type-II

$(GaAs)_m$ /$(AlAs)_m$ QWs with m = 5 to 13 monolayers, assuming the high-density e-h pairs. The correlation energy is evaluated by adopting RPA of Hubbard. The main difference of type-II GaAs/AlAs QWs with type-I structure is the partial confinement of electrons and holes into the wells which are separated spatially. It may produce the characteristic contributions to the e-h correlation as well as the electrostatics. In order to demonstrate the non-local nature of such charge neutrality, we examine the layer-thickness dependence of ground state energy of the EHL. In addition to these, we explore the stability of the EHL through the calculation of the binding energy in type-I and type-II $(GaAs)_m/(AlAs)_m$ QWs by changing m (layer-thickness). Our results indicate that the EHL in type-II QWs is more stable state than the exciton and biexciton, while the EHL is unstable in type-I QWs.

This paper is organized as follows. In § 2, the model and energy of the EHL will be described. In § 3, we will clarify the layer-thickness dependence of ground state energy of EHL and make a comparison of the EHL in type-II and type-I GaAs/AlAs QWs based on the numerical results. Final section § 4 will be devoted to concluding remarks.

2. Model and Energy of Electron-Hole Liquid

We model $(GaAs)_m/(AlAs)_m$ QWs as that the well widths for electron and hole are determined by the number of monolayers (m), and the barrier height for electron and hole is given by V_e and V_h, respectively, as shown in Fig. 1. The z-axis is chosen along the growth direction, and the origin of the z-axis is taken at the center of the well for electrons. It is known that electrons occupy the X_z state in AlAs layer and holes the Γ state in GaAs layer in type-II $(GaAs)_m/(AlAs)_m$ QWs, while the electrons are in the Γ state of GaAs layer in type-I QWs.[11] The electron energy surface at the X_z state of AlAs layer is an ellipsoid of revolution with a two-fold degeneracy so $m_{e,z}$ and $m_{e,xy}$ being the longitudinal and transverse electron effective mass, respectively. The in-plane 2D dynamics of electrons is determined by $m_{e,xy}$, and the motion in a confinement potential along the z-axis is described by $m_{e,z}$. For simplicity of formulation and discussion for type-II QWs, we ignore the two-fold degeneracy of electrons associated with the X_z states and adopt a single valley model for electron and hole as that the lowest conduction and heavy-hole valence subbands are occupied by electrons and holes with pair-density N, respectively. We will calculate the Coulomb energies in which the extent of the wave functions in QWs along z-axis is taken into account.

The total energy per e-h pair E_{tot} relative to separated electrons and holes at rest for the zero-temperature is written as

$$E_{tot} = E_{kin} + E_X + E_H + E_C. \qquad (1)$$

The average kinetic energy per e-h pair E_{kin} is

$$E_{kin} = \frac{1}{2}(\frac{\hbar^2 f_{e^2}}{2m_{e,xy}} + \frac{\hbar^2 f_h^2}{2m_h}), \tag{2}$$

where f_h (f_e) is the Fermi wave number of hole (electron) and m_h is the heavy hole effective mass.

The exchange energy E_X in eq.(1) is

$$E_X = E_X^{(e)} + E_X^{(h)}. \tag{3}$$

The exchange energy per hole $E_X^{(h)}$ can be calculated by

$$E_X^{(h)} = -N^{-1}(2\pi)^{-4} \int\int_{|\mathbf{k}|,|\mathbf{k}'|\leq f_h} d\mathbf{k}d\mathbf{k}' v_{hh}(|\mathbf{k}-\mathbf{k}'|), \tag{4}$$

where $\mathbf{k}=(k_x, k_y)$, and $v_{hh}(q)$ denotes the Fourier component of Coulomb interaction between holes. The Coulomb interaction components among electrons, holes, and between e-h are written by

$$v_{ij}(q) = \frac{2\pi e^2}{\epsilon q} \int_{-\infty}^{+\infty} dz \int_{-\infty}^{+\infty} dz' e^{-q|z-z'|} |\psi_i(z)|^2 |\psi_j(z')|^2 \quad (i,j = \mathrm{e,h}), \tag{5}$$

with dielectric constant ϵ and the wave function of the lowest subband $\psi_i(z)$. The exchange energy for electrons $E_X^{(e)}$ has a similar form with eq.(4), and is evaluated.[9]

In bulk and type-I structure, the Hartree energy is negligibly small because of the local charge neutrality between electrons and holes. But in type-II structure, this energy plays important role. The Hartree energy E_H in eq.(1) becomes

$$E_H = (2N)^{-1} \int_{-\infty}^{+\infty} dz \phi(z) \rho(z), \tag{6}$$

where the electrostatic potential $\phi(z)$ is obtained by solving the Poisson's equation with use of the charge density

$$\rho(z) = -eN(|\psi_e(z)|^2 - |\psi_h(z)|^2). \tag{7}$$

We will evaluate the correlation energy E_C for QWs by adopting RPA of Hubbard,[19] which is written as

$$\begin{aligned} E_C = &-\frac{\hbar}{4\pi^2 N} \int_0^{\infty} q dq \int_0^{\infty} d\omega \int_0^1 \frac{d\lambda}{\lambda} \mathrm{Im}[\epsilon^{-1}(\mathbf{q},\omega)] \\ &- \frac{1}{2(2\pi)^2} \int d\mathbf{q}[v_{ee}(q) + v_{hh}(q)] - E_X. \end{aligned} \tag{8}$$

The inverse dielectric function $\epsilon^{-1}(\mathbf{q},\omega)$ in eq.(8) is related to the proper polarization of electrons and holes W_{ii} (i = e, h) and the screened Coulomb interactions V_{ii} as follows,

$$\epsilon\epsilon^{-1}(\mathbf{q},\omega) = 1 - \epsilon[V_{ee}(\mathbf{q},\omega)W_{ee}(\mathbf{q},\omega) + V_{hh}(\mathbf{q},\omega)W_{hh}(\mathbf{q},\omega)]. \tag{9}$$

The functions V_{ii} accord to the coupled integral equations which are transform into the following algebraic Dyson's equations depicted by the diagrams in Fig. 2. They are given by

$$\begin{pmatrix} V_{\rm ee}(\mathbf{q},\omega) & V_{\rm eh}(\mathbf{q},\omega) \\ V_{\rm he}(\mathbf{q},\omega) & V_{\rm hh}(\mathbf{q},\omega) \end{pmatrix} = \lambda \begin{pmatrix} v_{\rm ee}(q) & v_{\rm eh}(q) \\ v_{\rm he}(q) & v_{\rm hh}(q) \end{pmatrix} + \lambda \begin{pmatrix} v_{\rm ee}(q) & v_{\rm eh}(q) \\ v_{\rm he}(q) & v_{\rm hh}(q) \end{pmatrix} \begin{pmatrix} W_{\rm ee}(\mathbf{q},\omega) & 0 \\ 0 & W_{\rm hh}(\mathbf{q},\omega) \end{pmatrix} \begin{pmatrix} V_{\rm ee}(\mathbf{q},\omega) & V_{\rm eh}(\mathbf{q},\omega) \\ V_{\rm he}(\mathbf{q},\omega) & V_{\rm hh}(\mathbf{q},\omega) \end{pmatrix}. \tag{10}$$

In order to take the exchange correction into account, we replace W by W' as

$$W'_{ii}(\mathbf{q},\omega) = \frac{W_{ii}(\mathbf{q},\omega)}{1+G_i(q)\lambda v_{ii}(q)W_{ii}(\mathbf{q},\omega)}, \tag{11}$$

where $G_i(q)$ (i = e, h) denotes the so-called exchange correction suggested by Hubbard,[19]

$$G_i(q) = v_{ii}((q^2+f_i^2)^{1/2})/2v_{ii}(q). \tag{12}$$

For calculation of E_C we assume the isotropic Fermi surface of electron with effective mass m_e. So finally we can cast into E_C as

$$E_C = \frac{\hbar}{4\pi^2 N}\int_0^\infty q dq \int_0^\infty d\omega \int_0^1 \frac{d\lambda}{\lambda} \times [\frac{\beta S - \alpha T}{\alpha^2+\beta^2} + v_{\rm ee}(q)\Sigma_{\rm e}(q,\omega)\lambda + v_{\rm hh}(q)\Sigma_{\rm h}(q,\omega)\lambda], \tag{13}$$

where

$$\begin{aligned}
\alpha &= 1 + \{(G_{\rm e}-1)v_{\rm ee}A_{\rm e} + (G_{\rm h}-1)v_{\rm hh}A_h\}\lambda \\
&\quad + \{(1-G_{\rm e})(1-G_{\rm h})v_{\rm ee}v_{\rm hh} - v_{\rm eh}^2\}(A_{\rm e}A_{\rm h} - \Sigma_{\rm e}\Sigma_{\rm h})\lambda^2, \\
\beta &= \{(G_{\rm e}-1)v_{\rm ee}\Sigma_{\rm e} + (G_{\rm h}-1)v_{\rm hh}\Sigma_{\rm h}\}\lambda \\
&\quad + \{(1-G_{\rm e})(1-G_{\rm h})v_{\rm ee}v_{\rm hh} - v_{\rm eh}^2\}(A_{\rm e}\Sigma_{\rm e} + A_{\rm h}\Sigma_{\rm h})\lambda^2, \\
S &= (v_{\rm ee}A_{\rm e} + v_{\rm hh}A_{\rm h})\lambda + \{(G_{\rm e}+G_{\rm h}-2)v_{\rm ee}v_{\rm hh} + 2v_{\rm eh}^2\}(A_{\rm e}A_{\rm h} - \Sigma_{\rm e}\Sigma_{\rm h})\lambda^2, \\
T &= (v_{\rm ee}\Sigma_{\rm e} + v_{\rm hh}\Sigma_{\rm h})\lambda + \{(G_{\rm e}+G_{\rm h}-2)v_{\rm ee}v_{\rm hh} + 2v_{\rm eh}^2\}(A_{\rm e}\Sigma_{\rm e} + A_{\rm h}\Sigma_{\rm h})\lambda^2.
\end{aligned} \tag{14}$$

In eqs.(13) and (14), $A_{\rm e}$ ($A_{\rm h}$) and $\Sigma_{\rm e}$ ($\Sigma_{\rm h}$) are the real and imaginary parts of the 2D electron (hole) polarizability in RPA, respectively, as

$$A_i(q,\omega) = \frac{m_i}{\pi\hbar^2 q}[(\frac{m_i\omega}{\hbar q}+\frac{q}{2})\sqrt{1-(\frac{2\hbar f_i q}{2m_i\omega+\hbar q^2})^2} - (\frac{m_i\omega}{\hbar q}-\frac{q}{2})\sqrt{1-(\frac{2\hbar f_i q}{2m_i\omega-\hbar q^2})^2} - q], \tag{15}$$

$$\Sigma_i(q,\omega) = \frac{m_i}{\pi\hbar^2 q}\left[\sqrt{f_i^2 - (\frac{m_i\omega}{\hbar q} + \frac{q}{2})^2} - \sqrt{f_i^2 - (\frac{m_i\omega}{\hbar q} - \frac{q}{2})^2}\right], \tag{16}$$

where $i =$ e, h ($m_e = m_{e,xy}$) and $\sqrt{x} = 0$ when $x < 0$. In the above E_C, we account e-e, h-h and e-h correlation effects in the RPA of Hubbard. In type-I QWs,[9] the exchange correction for e-h system are considered for $\Sigma_e + \Sigma_h$ and $A_e + A_h$ because the Coulomb interactions are approximated by the same form, and the integral over λ is evaluated easily. However, since in the present case v_{ij} (i, $j =$ e, h) differ each other, these remain explicitly in the integration over λ.

To proceed the numerical studies of the EHL, we define the minimum in E_{tot} as a function of e-h pair density as the ground state energy E_G per e-h pair i.e.

$$E_G = -\min[E_{tot}(N)]. \tag{17}$$

The corresponding equilibrium pair-density is set to be N_0. Further we introduce the binding energy of the EHL E_{bin} to discuss the stability of the EHL as

$$E_{bin} = E_G - B_X - \frac{1}{2}B_{XX} \tag{18}$$

where B_X and B_{XX} are the binding energy of exciton and biexciton, respectively. It is known that the many-body effect reduces significantly the band-gap. This so-called band-gap renormalization (BGR) E_{BGR} is defined as

$$E_{BGR} = d[N(E_X + E_H + E_C)]/dN. \tag{19}$$

3. Results and Discussion

3.1 Layer-Thickness Dependence of Ground State Energy in Type-II GaAs/AlAs QWs

We calculate the total energy of quasi-2D EHL for type-II GaAs/AlAs QWs according to formulae in § 2. We employ the standard parameters of type-II GaAs/AlAs QWs such as $m_{e,z} = 1.1m_0$, $m_{e,xy} = 0.19m_0$, $m_h = 0.51m_0$, $\epsilon = 11.17$, $V_e = 300$ meV and $V_h = 550$ meV. The lattice constant is assumed to be $a = 5.6533$Å. To see various contributions in E_{tot}, we plot E_{kin}, E_X, E_H, E_C together with E_{tot} as a function of pair-density N for type-II $(GaAs)_{10}/(AlAs)_{10}$ QWs in Fig. 3. The layer-thickness dependence[22] of E_G is found by changing the number of monolayers. In Fig. 4, E_{tot} is shown as a function of N in type-II $(GaAs)_m/(AlAs)_m$ QWs for $m = 5$, 7, 10 and 13. It is evident that E_G appears at the lower equilibrium pair density with smaller magnitude (i.e. smaller $|E_G|$) as the well thickness is increased. This is due to an increase of E_H, a decrease of $|E_X|$ and $|E_C|$, and independence of thickness in E_{kin} when the thickness is increased. The increase of E_H is understood by the Gauss's law. The reduction of $|E_X|$ is due to that the Coulomb interactions v_{ee} and v_{hh} become strong as the width of wells increases. It should be noted that $|E_C|$ does not contribute to the determination of N_0 almost because of its weak N-dependence, while it reduces E_{tot} significantly.

Figure 5 exhibits the BGRs versus N in type-II $(GaAs)_m/(AlAs)_m$ QWs for m = 5(a), m = 7(b), m = 10(c) and m =13(d). The BGRs for m = 5(a) and 7(b) decrease monotonously as N increases. However the BGRs for m = 13(d) decreases gradually in low density region as N increases, and it reaches a minimum value and then starts to increase. This tendency is seen also in the curve (c) for $m = 10$. The behavior of curve (d) is ascribed to the increase of E_H at high density region. At high density, Hartree field will compensate the confined potential and the band-gap will increase with e-h pair-density.

3.2 Comparison of EHL in Type-II GaAs/AlAs QW with Type-I Structures

In order to demonstrate the characteristic of the EHL in type-II structure, we plot E_{tot} for type-II and type-I QWs by changing layer-thickness in Fig. 6. The lines (a), (b) and (c) stand for E_{tot} as a function of N for $(GaAs)_{10}/(AlAs)_{10}$ QWs and $(GaAs)_m/(AlAs)_m$ QWs with m = 17 and 20, respectively. We have used $m_e = 0.067m_0$, $m_h = 0.51m_0$, $\epsilon = 11.17$, V_e = 1060 meV and V_h = 550 meV for type-I GaAs/AlAs QWs. It is quite interesting that E_G and N_0 change dramatically from type-II to type-I QWs. This is mainly attributed to the increase of E_{kin} due to the light effective mass of electron in type-I QWs. In the present results, the e-e and h-h Coulomb interactions play a similar role for both type-I and type-II QWs and the difference of Fermi surface between type-II and typ-I structures does not produce a large change in the summations over k and k' in E_X, so the exchange energy does not change much consequently. E_H is almost zero in type-I QWs, since the local cancellation of charges between electrons and holes takes place. We note that $|E_C|$ becomes small in type-I structure compared with that of type-II, it does not depend on N almost, and plays a minor role to determine N_0.

According to our definition of E_{bin} in eq.(19), the EHL will be formed if E_{bin} is positive. E_{bin} in $(GaAs)_m/(AlAs)_m$ QWs with m = 5-13 for type-II QWs, and m = 14,19, and 20 for type-I QWs are plotted by closed and open circles, respectively, in Fig. 7. B_X and B_{XX} in eq.(19) are calculated by the quantum Monte Carlo method.[23-25] Since type-II QWs appear when $m \leq 13$, and the systems become type-I structure for $m \geq 14$, it is expected that the quasi-2D EHL will be formed apparently in type-II GaAs/AlAs QWs, while it does not be formed in type-I QWs. Here we point out that the steep drop in E_{bin} from type-II to type-I QWs is attributed to the decrease of $|E_G|$ as is seen from Fig. 6 because B_X and B_{XX} do not change much between structures in type-I and type-II QWs.

Finally we compare our calculation of E_{tot} with previous result in type-I $GaAs/Ga_{1-x}Al_xAs$ QWs with well width 145 Å.[10] Our calculated energy for $x = 0.3$ is E_G = 8.4 meV for N_0 = 1.55 $\times$ 10^{11} cm^{-2}. These are close to the E_G and N_0 in ref. 8.

4. Concluding remarks

We have explored the ground state energy of quasi-2D EHL for type-II GaAs/AlAs QWs in comparison with that of type-I GaAs/AlAs QWs by adopting the RPA of Hubbard for the correlation energy. It is concluded that the quasi-2D EHL is more stable state than exciton and biexciton at high e-h pair density in type-II $(GaAs)_m/(AlAs)_m$ QWs ($5 \leq m \leq 13$) while the EHL is unstable in type-I QWs ($m \geq 14$). Associated with these conclusions is that the binding energy and the equilibrium density of EHL are changed drastically when a switching from a type-II to a type-I structure takes place in $(GaAs)_m/(AlAs)_m$ QWs at a critical thickness.

In the present paper, we assumed that the EHL in type-II QWs consists of both the electrons at the X_z-point in AlAs layer and holes at the Γ-point in GaAs QW, whereas the electrons at Γ-point in GaAs QW contribute to the formation of EHL in type-I case. In the near vicinity of critical thickness, the more complete consideration of the band structures in GaAs/AlAs QWs should be required to calculate the EHL energy. As was described at first, the single-valley is assumed for electron and hole. The many-valley effects were ignored in the present correlation energy calculation because the electron population at many valleys will lead further complexity, so that we neglected these in the other energy calculations for the sake of consistency. To examine effects of many-valleys, we estimate numerically $E_0 = E_{kin} + E_X + E_H$ for type-II $(GaAs)_m/(AlAs)_m$ QWs by taking two-valley effects into account. It is found that the minimum value of our calculated E_0 increases a little compared with the results in single-valley model (the increment of E_0 is about 1.4 meV ($m = 5$) $\sim$ 0.4 meV ($m = 13$)), so that the corresponding density at minimum E_0 exhibits a small decrease. The reduction is about 1.5×10^{12} cm^{-2} ($m = 5$) $\sim 0.5 \times 10^{12}$ cm^{-2} ($m = 13$). Since the numerical evaluation of E_C is difficult for many valley structures even for two-valleys case, and it was pointed out already by Vashishta et al.[3] that $|E_C|$ increases slightly when the many-valleys effect is considered, so we believe that our conclusions obtained in the present approximation do not be changed much even if many-valleys were taken into account. Finally, we comment recent observations of condensation of indirect excitons in biased coupled AlAs/GaAs quantum wells in a strong magnetic field.[14,15] This exciton condensation corresponds to the k-space ordering, while our EHL occurs in the real-space. In the Hubbard approximation for a high density e-h system,[20] we did not take into account the multiple e-h scattering in higher-order correlation which leads to the formation of excitons. So the connection between the EHL and excitonic condensation is not clear. However, this suggests us that the e-h pair fluctuation which was partially contained in our calculation as a dynamical screening in the Hubbard approximation may play important role in the transition from dilute to high density regime of e-h pair density. It is strongly expected that the many-body interaction among particles in e-h system should be studied in a controlled manner in type-II quantum wells.

Acknowledgements

The authors would like to thank Professor T. Tsuchiya for helpful discussions and for providing the numerical data of the binding energies of exciton and biexciton by the quantum Monte Carlo calculations.

1) T. M. Rice: *Solid State Physics*, ed. H. Ehrenreich, F. Seitz and D. Turnbull (Academic, New York, 1977) Vol. 32, p.1.
2) J. C. Hensel, T. G. Phillips and G. A. Thomas: *Solid State Physics*, ed. H. Ehrenreich, F. Seitz and D. Turnbull (Academic, New York, 1977) Vol. 32, p.88.
3) P. Vashishta, R. K. Kalia and R. S. Singwi: *Electron-Hole Droplets in Semiconductors*, ed. C. D. Jeffries and L. V. Keldysh (North-Holland, Amsterdam, 1983) p.1.
4) L. V. Keldysh: *Proc. 9th Int. Conf. Phys. Semiconductors, Moscow* (1968) p.1303.
5) M. Nagai, R. Shimano and M. Gonokami: Phys. Rev. Lett. **86** (2001) 5795.
6) R. Shimano, M. Nagai, K. Horiuch and M. Gonokami: Phys. Rev. Lett. **88** (2002) 057404.
7) See the book by A. Isihara: *Electron Liquids* (Springer-Verlag, Berlin, 1998) 2nd ed., Chap.5, p.71 [in English].
8) See the review article by R. Cingolani and K. Ploog: Adv. Phys. **40** (1991) 535 and references therein.
9) D. A. Kleinman: Phys. Rev. B **33** (1986) 2540.
10) G. E. W. Bauer and T. Ando: Phys. Rev. B **34** (1986) 1300.
11) See for example, M. Nakayama, I. Tanaka, I. Kimura and H. Nishimura: Jpn. J. Appl. Phys. **29** (1990) 41.
12) H. Kalt, R. Nötzel and K. Ploog: Solid State Commun. **83** (1992) 285.
13) K. Boujdaria, D. Scalbert and C. Benoit À La Guillaume: Phys. Stat. Sol. (b) **183** (1994) 309.
14) L. V. Butov, A. Zrenner, G. Abstreiter, G. Böhm and G. Weimann: Phys. Rev. Lett. **73** (1994) 304.
15) L. V. Butov and A. I. Filin: Phys. Rev. B **58** (1998) 1980.
16) I. V. Lerner and Yu. E. Lozovik: Sov. Phys. JETP **53** (1981) 763.
17) Y. Kuramoto and C. Horie: Solid State Commun. **25** (1978) 713.
18) P. Hawrylak: Phys. Rev. B **39** (1989) 6264.
19) J. Hubbard: Proc. R. Soc. London, Ser. A **243** (1957) 336.
20) W. F. Brinkman and T. M. Rice: Phys. Rev. B **7** (1972) 1508.
21) Y. Kuramoto and H. Kamimura: J. Phys. Soc. Jpn **37** (1974) 716.
22) A. Inagaki and S. Katayama: Solid State Commun. **125** (2003) 337.
23) T. Tsuchiya: private communication.
24) T. Tsuchiya and S. Katayama: Physica B. **249-251** (1998) 612.
25) B. L. Hammond, W. A. Lester, Jr. and P. J. Reynolds: *Monte Carlo Methods in ab initio Quantum Chemistry* (World Scientific, Singapore, 1994) p.77 [in English].

Fig. 1. Schematic view of type-II QWs.

Fig. 2. Summation of polarization diagrams in the RPA. v_{ij} and V_{ij} denote the bare Coulomb and screened interactions. W_{ii} displays the proper polarization part.

Fig. 3. E_{kin}, E_X, E_H, E_C and E_{tot} vs e-h pair-density N in type-II $(GaAs)_{10}/(AlAs)_{10}$ QWs.

Fig. 4. E_{tot} vs N in type-II $(GaAs)_m/(AlAs)_m$ QWs with $m = 5$, 7, 10 and 13.

Fig. 5. E_{BGR} vs N in type-II $(GaAs)_m/(AlAs)_m$ QWs with $m = 5$ (a), $m = 7$ (b), $m = 10$ (c) and $m = 13$ (d) .

Fig. 6. E_{tot} vs N in $(GaAs)_m/(AlAs)_m$ QWs with $m = 10$ (a), $m = 17$ (b) and $m = 20$ (c).

Fig. 7. Binding energy of EHL E_{bin} in $(GaAs)_m/(AlAs)_m$ QWs for numbers of monolayers m.

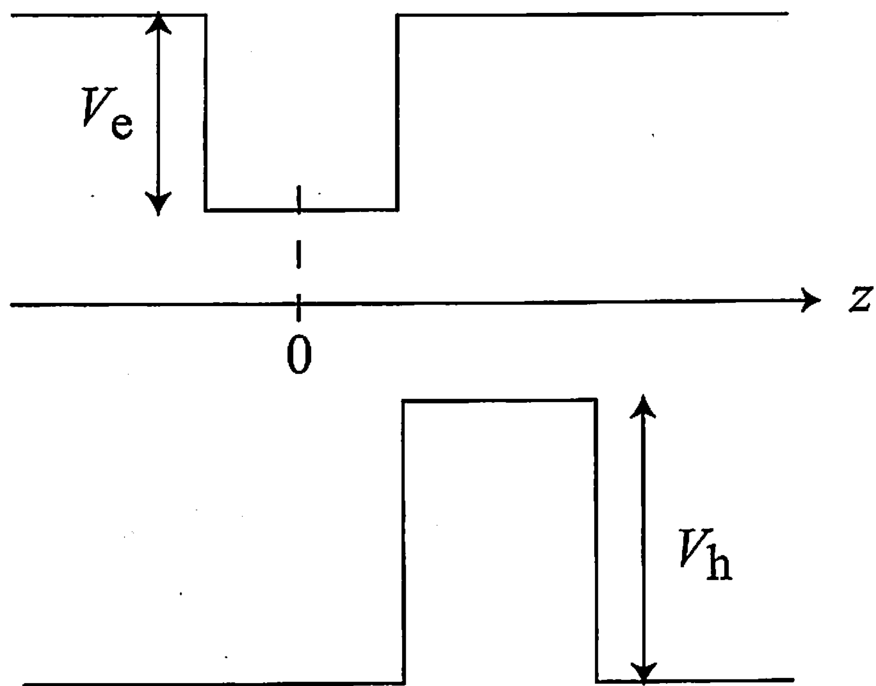

Fig. 1 （横幅 8cm）

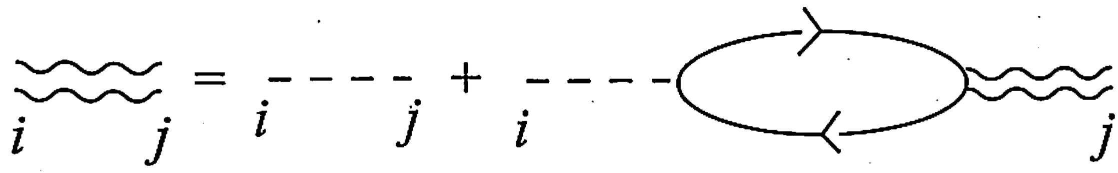

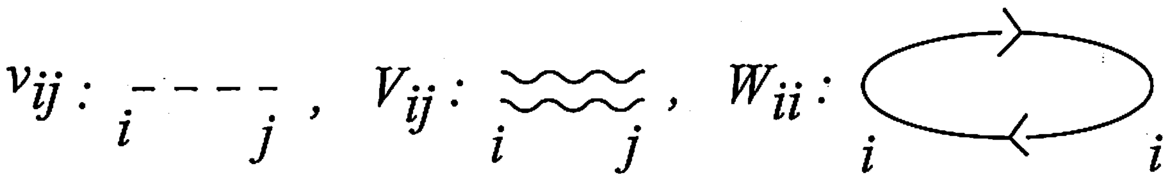

Fig. 2 (横幅 8cm)

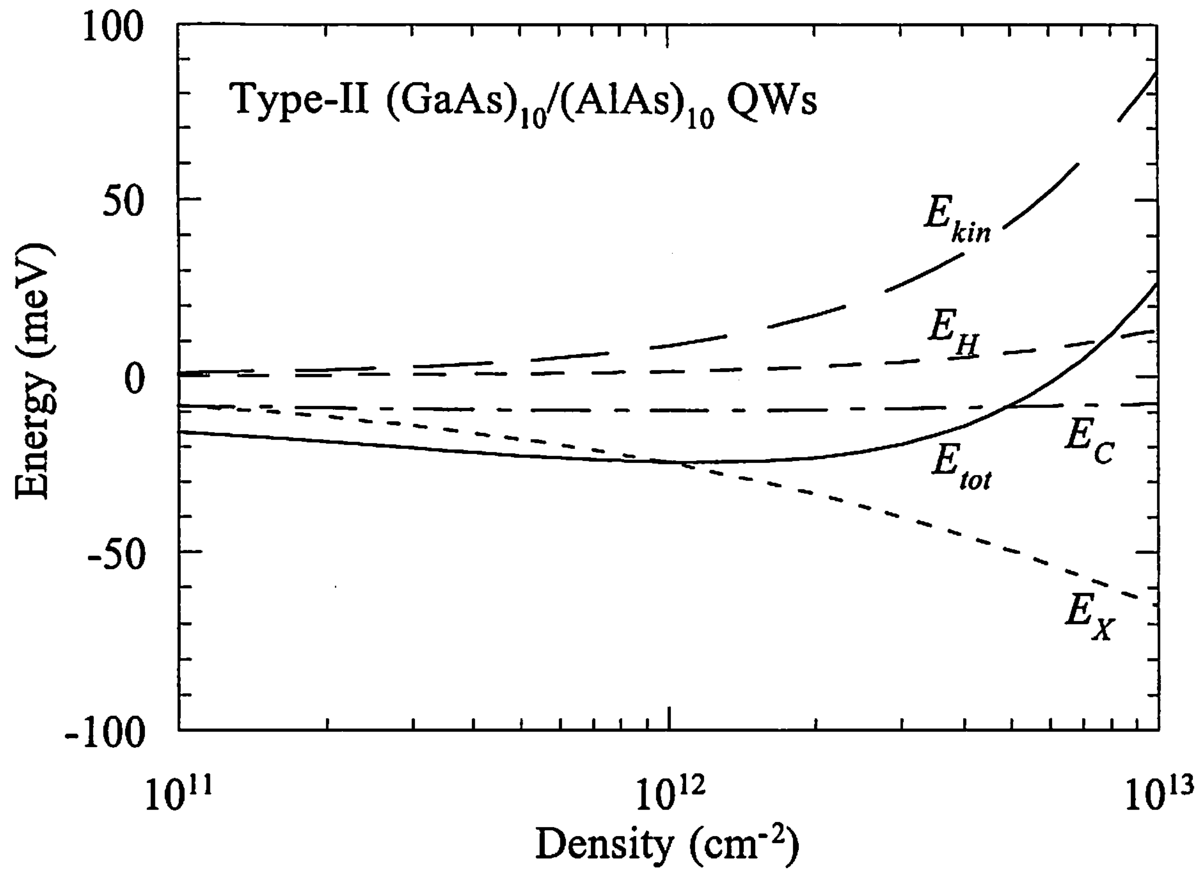

Fig. 3 (横幅 8.3 cm)

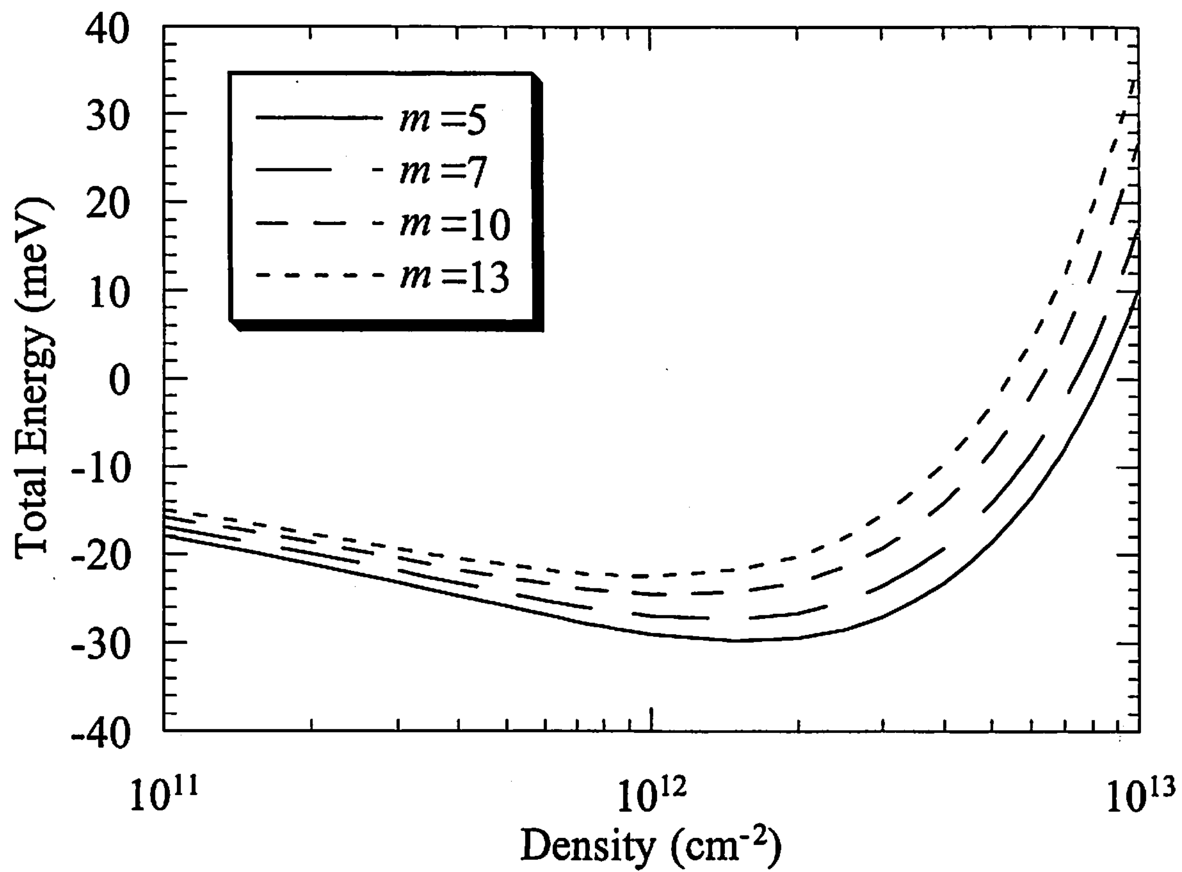

Fig. 4 （横幅 8.3 cm）

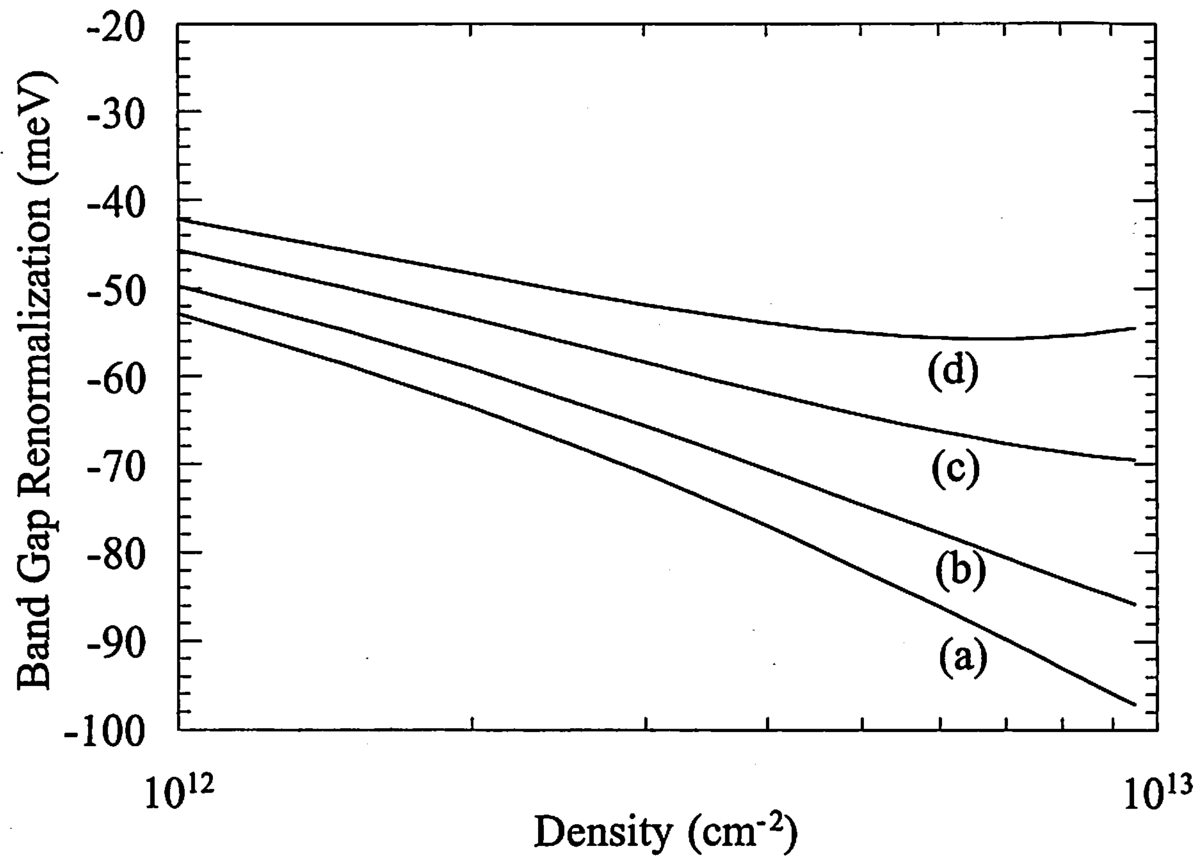

Fig. 5 (横幅8.3cm)

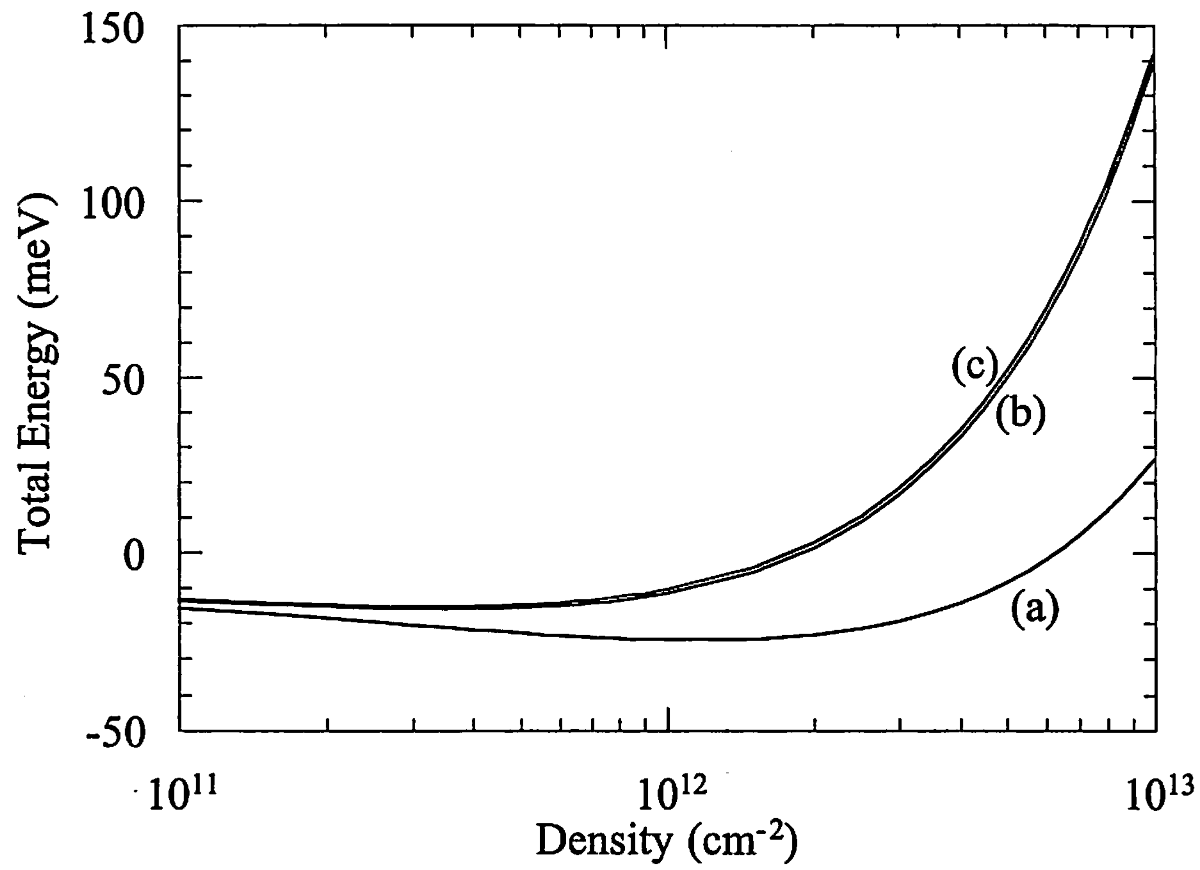

Fig. 6 (横幅 8-3 cm)

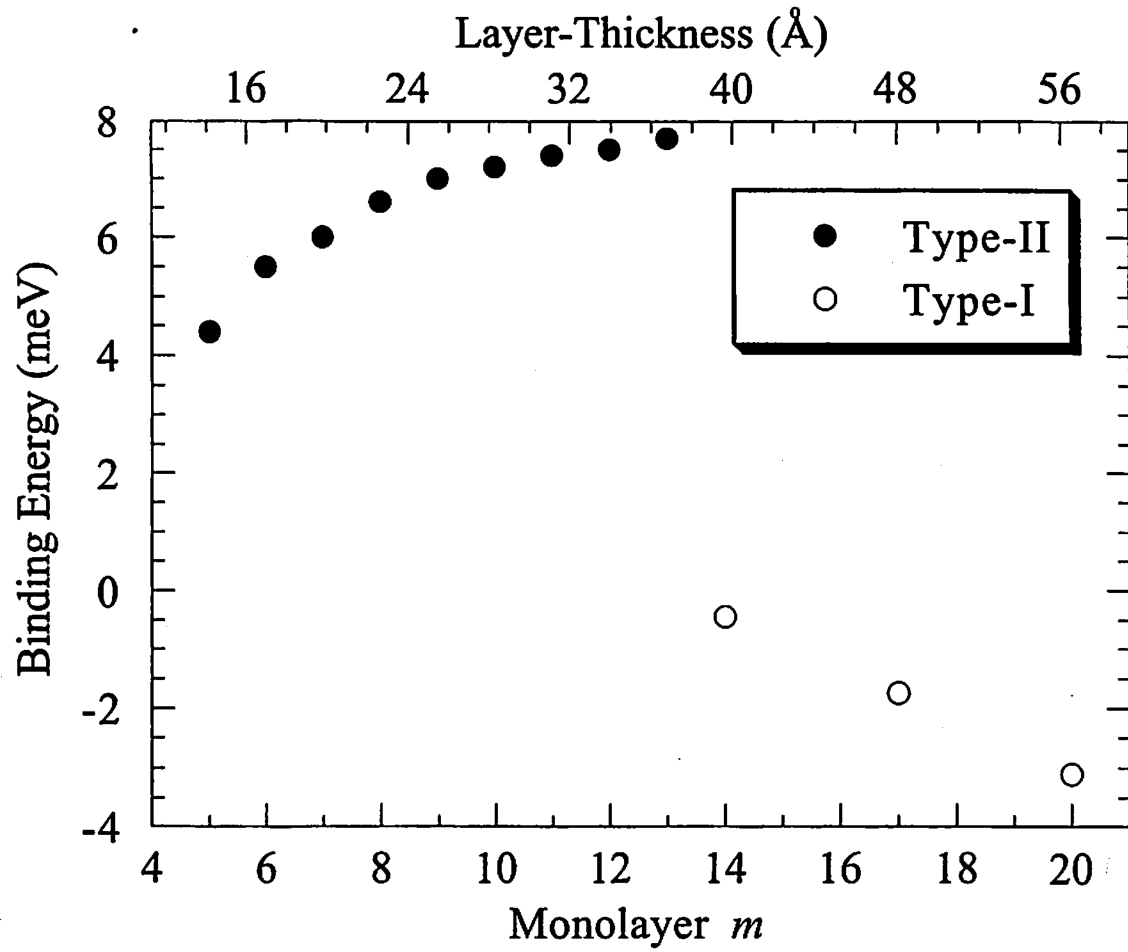

Fig. 7 (横幅 8.3 cm)